

# Absence of enhanced superconductivity in double-barrier superconducting tunnel junctions: Measurements of lateral electric transport in the middle normal-metal layer

I. P. Nevirkovets and O. Chernyashevskyy

Department of Physics and Astronomy, Northwestern University, Evanston, Illinois 60208, USA  
and Institute for Metal Physics NASU, 03680 Kyiv, Ukraine

J. B. Ketterson

Department of Physics and Astronomy, Department of Electrical Engineering and Computer Science, and Materials Research Center,  
Northwestern University, Evanston, Illinois 60208, USA

(Received 3 May 2006; published 23 June 2006)

The lateral conductivity of the middle Al layer of a Nb/Al/AIO<sub>x</sub>/Al/AIO<sub>x</sub>/Al/Nb (SINIS) multiterminal device is studied as a function of the current injected perpendicular to the layers in a regime where a gap-difference-like feature is observed in the current-voltage characteristic. The response of the Al layer does not confirm an earlier reported observation of superconductivity in the Al far above its transition temperature [Blamire *et al.*, Phys. Rev. Lett. **66**, 220 (1991)].

DOI: 10.1103/PhysRevB.73.224521

PACS number(s): 74.45.+c, 74.50.+r, 74.78.Fk, 85.25.Am

## I. INTRODUCTION

Over the past several years, double-barrier superconducting tunnel junctions with the SINIS structure have been extensively studied, both theoretically and experimentally; here S, I, and N denote a superconductor, an insulator, and a normal metal, respectively.<sup>1-7</sup> SINIS junctions display interesting new features that are not observed in SIS or SNS junctions. A report by Blamire *et al.* of the observation of superconductivity far above the critical temperature of Al in a symmetric Nb/AIO<sub>x</sub>/Al/AIO<sub>x</sub>/Nb double-barrier tunnel junction attracted considerable theoretical attention.<sup>8</sup> The experiments revealed an anomalous feature in the current-voltage characteristic (CVC) of a SINIS junction similar to the well known gap-difference feature; Blamire *et al.* concluded that the Al energy gap persists up to temperatures as high as 4 K. Theoretical models of the effect were developed by Heslinga and Klapwijk<sup>9</sup> and by Zaitsev,<sup>10</sup> who explained the anomalous feature as being due to nonequilibrium quasiparticle extraction from the N layer when current passes across the structure for a certain range of voltages. This explanation is widely accepted in the field of nonequilibrium superconductivity.<sup>11</sup> It has even been predicted that superconductivity can be enhanced to arbitrarily high temperatures by tunneling extraction of quasiparticles in a *p*-type semiconductor/superconductor/*n*-type semiconductor structure,<sup>12</sup> although this prediction has been questioned.<sup>13</sup> Independently of these works, Leivo *et al.* considered electric and heat transport in SINIS junctions and suggested that the anomalous feature can be explained by an alternative mechanism.<sup>2</sup> On the other hand, a more detailed experimental study of the feature by one of the authors showed that the associated structure is more complex than the usual gap-difference feature, and questioned whether it results from the appearance of a gap in the Al, or is associated with some other anomaly in the tunneling density of states,<sup>14</sup> an interpretation that is supported theoretically.<sup>6</sup>

Although of potential fundamental importance, it appears that the feasibility of enhancing superconductivity via

nonequilibrium effects (at temperatures far above the equilibrium superconducting transition temperature,  $T_c$ ) remains controversial. Clearly, a direct measurement of the response of the N layer in an SINIS junction in the presence of a tunneling current is of key importance. In our former work, it was shown that lateral electrical transport in the middle Al layer of a multiterminal, double-barrier Nb/Al/AIO<sub>x</sub>/Al/AIO<sub>x</sub>/Al/Nb tunnel device can provide information on the actual state (superconducting or not) of the Al layer within the device.<sup>15</sup> In this paper, we report the lateral current transport in the presence of a vertical (perpendicular) tunneling current in the regime where the anomalous feature discussed above is observed.

## II. EXPERIMENT

The device fabrication procedures used have been described in some detail elsewhere.<sup>15,16</sup> The structures were deposited on *R*-plane sapphire substrates. Two sets of devices were fabricated and characterized which had different lateral sizes:  $L_t=11\ \mu\text{m}$ ,  $L_b=19\ \mu\text{m}$ , and  $W=10\ \mu\text{m}$ ; and  $L_t=12\ \mu\text{m}$ ,  $L_b=20\ \mu\text{m}$ , and  $W=14\ \mu\text{m}$  (here  $L_t$  and  $L_b$  denote the length of the top and bottom junction, respectively, and  $W$  denotes the width of the device, equal for the top and bottom junction; see Fig. 1). The thickness of the middle Al electrode,  $d_N$ , was varied in the range from 7 to 180 nm; the

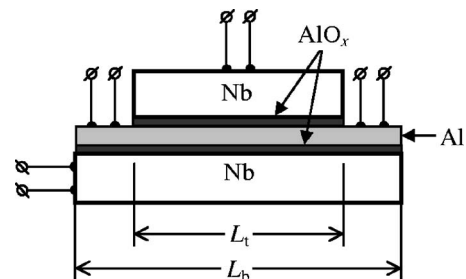


FIG. 1. Schematic cross-sectional view of a multiterminal SINIS device.

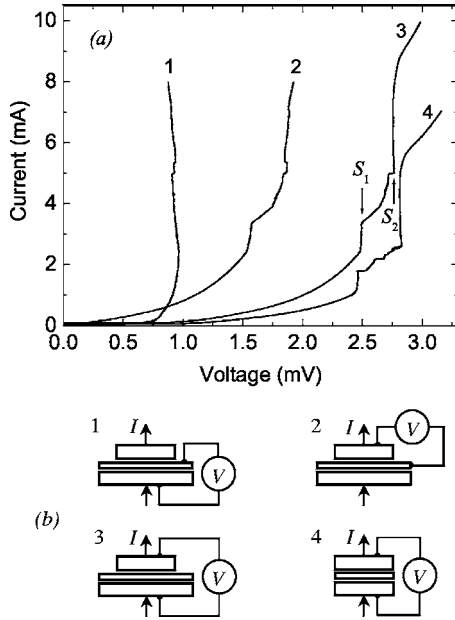


FIG. 2. (a) Current-voltage characteristics (CVC) of a multiterminal SINIS device (1–3) measured at 1.85 K for configurations 1–3, shown in (b). Arrows (down and up) denote “gap-difference” ( $S_1$ ) and “gap-sum” ( $S_2$ ) features in curve 3. Curve 4 is the CVC of a two-terminal SINIS junction (measured at 1.85 K) using configuration 4 in (b).

thickness of the Nb electrodes was 140–280 nm for the bottom layer and 110 nm for the top layer.

The transparency of the tunnel barriers was chosen so that the anomalous gap-difference-like feature<sup>8,14</sup> appeared in the measured CVC. The specific tunneling resistance,  $R_t$ , of our devices is about  $5 \times 10^{-7} \Omega \text{ cm}^2$ , which corresponds to the resistance range used in Ref. 8. The CVC of a representative device 1 with  $d_N=11$  nm,  $L_t=12 \mu\text{m}$ ,  $L_b=20 \mu\text{m}$ , and  $W=14 \mu\text{m}$  is shown in Fig. 2(a) at 1.85 K (curves 1–3); other devices showed qualitatively the same behavior. For these curves, the current passes perpendicular to the layers and voltage differences were measured across the bottom barrier (curve 1), the top barrier (curve 2), and the device as a whole (curve 3). The respective measurement configurations are shown in Fig. 2(b). To minimize electric noise, the experiments were carried out in a shielded room with a filtered electric power line; low-noise preamplifiers and battery-powered electronics were used to current bias the devices. The measurement system was capable of resolving a zero-voltage superconducting current of  $1 \mu\text{A}$  and even smaller changes in current.

### III. RESULTS AND DISCUSSION

One can see that the CVC of the device as a whole [curve 3 in Fig. 2(a)] exhibits two large steps,  $S_1$  and  $S_2$ . Similar steps for SINIS junctions were interpreted as gap-difference and gap-sum features.<sup>8</sup> We also note that a complex structure appears between these current steps; this additional structure should not appear for the SIS' case. Curve 4 shows the data for a two-terminal SINIS junction [(see measurement con-

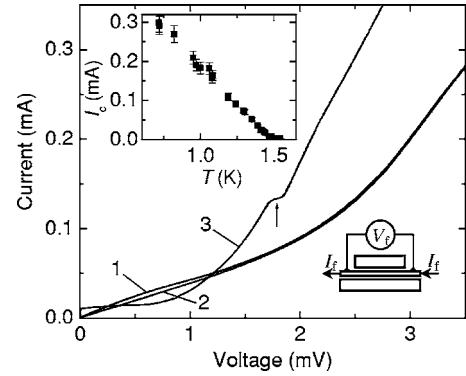


FIG. 3. The unperturbed  $I_f(V_f)$  curve of the N layer in device 1 in zero magnetic field (curve 1) and in an applied magnetic field of 35 Oe (curve 2). Curve 3 is the  $I_f(V_f)$  curve of the N layer in device 2 which has microshorts between N and S at one edge of the bottom NIS junction;  $T=1.85$  K. Upper inset:  $I_{cf}(T)$  dependence of N layer in device 3. Lower inset: schematic of the measurement configuration.

figuration 4 in Fig. 2(b)] that also shows the feature at  $V < 2\Delta_{\text{Nb}}/e$  (here  $\Delta_{\text{Nb}}$  is the superconducting energy gap of Nb) and an even stronger “between-gap” structure; the two-terminal junctions (with lateral dimensions  $10 \mu\text{m} \times 10 \mu\text{m}$ ) were fabricated identically with multiterminal devices and measured for reference. Depending on the junction parameters, the additional structure may be absent or not resolved in the experiments. From curves 1 and 2, one can see that the step features are displayed in the CVC of both the top and bottom junctions, but the main contribution to the  $S_1$  step in curve 3 is associated with the top junction. Note that when the contributions from the two junctions are summed, the  $S_1$  step in curve 3 is practically vertical.

We observed that the step  $S_1$  is a very elusive feature, and not only its shape, but even its presence is not well reproduced for junctions fabricated under similar conditions (and having the tunnel-specific resistance within the same range). One would expect the feature to be more robust if a nonequilibrium quasiparticle distribution was responsible for it.

The unperturbed  $I_f(V_f)$  curves for device 1 at 1.85 K are shown in Fig. 3 (see the schematic of the measurement configuration in the lower inset). Here, curve 1 was measured for  $H=0$ , whereas curve 2 was measured in a field of 35 Oe applied parallel to the layer plane. One can infer from these curves that the Al layer is dissipative,<sup>17</sup> however there is a small coherent contribution to the lateral conductivity of the Al layer, in accordance with our former observations.<sup>15</sup> At the same time, at 1.85 K, a Josephson current,  $I_c$ , of about  $100 \mu\text{A}$  was observed across the device [cf. Fig. 2(a), curves 1–3]. From curves 1 and 2, using the resistance at 1 mV, and taking into account the geometry of the Al layer, its resistivity is estimated to be  $19 \mu\Omega \text{ cm}$ , a value expected for a moderately dirty Al film.

We would like to emphasize that this kind of behavior is seen only in high-quality specimens. Weak spots in the barriers may result in a much stronger proximity effect and a supercurrent in the N layer. Curve 3 in Fig. 3 is the  $I_f(V_f)$  curve for the N layer in a SINIS device 2 identical to device 1, but with a direct electric contact between N and S at one

edge of the bottom NIS junction (as established from voltage measurements at the two edges while passing the current across all the layers: above  $I_c$ , the voltage was close to zero at one edge, and finite at the other edge). Although such a direct electric contact does not affect the CVC of the device 2 as a whole (so that its CVC is very similar to the curve 3 in Fig. 2), dramatic changes occur in its  $I_f(V_f)$  curve in comparison with the  $I_f(V_f)$  curve for the device 1: (i) the gap-sum feature in curve 3 appears at a voltage approximately half of that for curves 1 and 2 (cf. Fig. 3), because the current crosses the tunnel barriers only once (the reason why the gap-sum feature appears in the CVC of the N layer is explained in Ref. 15); (ii) a zero-voltage supercurrent,  $I_{cf}$ , of about  $11 \mu\text{A}$  and a gap-difference feature (marked by an arrow in Fig. 3) appear in curve 3. Similar CVC (with the supercurrent and a gap-difference feature) was observed for devices where no Zr layer was deposited in the current leads to the middle Al layer; this Zr layer serves to prevent the proximity between the topmost Nb layer and the underlying Al.<sup>15,16</sup>

To fully understand the shape of the curve 3 (as well as curves 1 and 2), a detailed theoretical description of the system is necessary. Qualitatively, it is clear that there is some contribution to the CVC of the Al layer from the transport through an S/weak-link/S' junction formed at one edge of the film (here S' denotes a proximitized Al). Since the superconducting energy gap is now developed in Al by a strong proximity effect through a weak link, the gap-related features (such as a reduced conductivity at low bias and the gap-difference feature) may appear in the CVC. On the other hand, an increased conductivity in the subgap region and the absence of the gap-difference feature in curves 1 and 2 are consistent with a view that in this case a stable order parameter is not induced in the Al film. This experimental observation implies that (i) although a direct electric contact between N and S is present at one edge, the coherence spreads over the entire length of the Al film, i.e., over a distance (governed by the diffusion length that is typically of the order of  $10 \mu\text{m}$  for metallic films at low temperatures) considerably longer than the coherence length, in accordance with earlier observations on mesoscopic systems,<sup>18</sup> and (ii) possibly, there is a critical S/N barrier strength below which the fluctuating superconductivity turns into an ordinary superconductivity.

To further clarify how the superconductivity (if present) in the N layer modifies its CVC, we carried out the  $I_f(V_f)$  and  $I_{cf}(T)$  measurements down to  $0.7 \text{ K}$  for a device 3 with parameters very close to those of device 1 but with  $d_N=14 \text{ nm}$ . The  $I_{cf}(T)$  dependence is shown in the top inset of Fig. 3; a parallel magnetic field of  $50 \text{ Oe}$  was applied to suppress a weak superconductivity. A measurable zero-voltage current was detected at  $1.55 \text{ K}$ , assumed to be the  $T_c$  of the Al film. With this  $T_c$  value, using the BCS relation  $2\Delta_{\text{Al}}/kT_c=3.52$ , we obtain  $\Delta_{\text{Al}}=0.23 \text{ meV}$ . If the step  $S_1$  in curve 3 [cf. Fig. 2(a)] is the gap difference, then it corresponds to  $\Delta_{\text{Al}}=0.14 \text{ meV}$ . Assuming that the critical current densities of the N layers in the devices 1 and 3 are the same (which is reasonable because the devices were fabricated in the same deposition run under the same conditions), and

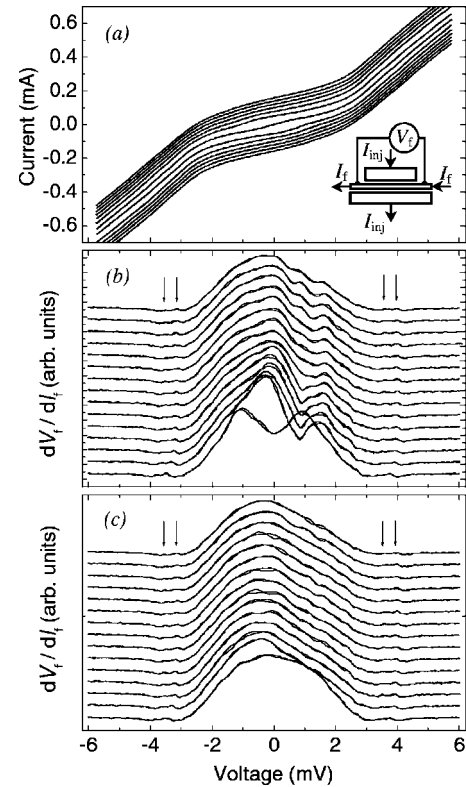


FIG. 4. (a) A family of CVC,  $I_f(V_f)$ , for the middle Al layer at various injection levels,  $I_{inj}$ . Curves from top to bottom are for  $I_{inj}=-8.0, -4.0, -3.0, -2.0, -1.0, -0.2, 0.0, +0.2, +1.0, +2.0, +3.0, +4.0$ , and  $+8.0 \text{ mA}$ , respectively, and are shifted from each other by  $0.02 \text{ mA}$  along the current axis for clarity. Positive directions for currents  $I_{inj}$  and  $I_f$  are defined in the inset. The differential resistance of the middle Al layer under various  $I_{inj}$  levels is shown for zero applied magnetic field (b) and for an applied magnetic field of  $35 \text{ Oe}$  (c).  $dV_f/dI_f(V_f)$  curves from bottom to top (successively shifted upward from each other for clarity) are for  $I_{inj}=0, 0.2, 0.4, 0.6, 0.8, 1.0, 2.0, 2.2, 2.5, 2.8, 3.0, 3.5, 4.0, 6.0$ , and  $8.0 \text{ mA}$ , respectively.

making use of the  $I_{cf}(T)$  dependence and the BCS  $\Delta_{\text{Al}}(T)$  dependence, we obtain that for  $\Delta_{\text{Al}}=0.14 \text{ meV}$  the N layer in device 1 should carry a supercurrent of at least  $50 \mu\text{A}$  (the same estimation gives  $200 \mu\text{A}$  in zero magnetic field). Such a current is well above the resolution capability of the measurement technique and its appearance should be detected in the CVC of the Al film.

We next consider how an injection current,  $I_{inj}$ , passing perpendicular to the layers, affects lateral current transport in the middle Al layer. (In this experiment, we used two independent current sources with floating grounds.) When  $I_{inj}$  reaches the region of the “gap-difference” feature [i.e.,  $2.4\text{--}5.0 \text{ mA}$ ; cf. curve 3 in Fig. 2(a)], one would expect dramatic changes in  $I_f(V_f)$  due to the conjectured transition of the Al layer (or at least its portion situated inside the stack) into a superconducting state, such as an increase of the coherent contribution to the current (or even appearance of zero-voltage current), and, possibly, changes in the gap-related features. In Fig. 4(a), a family of  $I_f(V_f)$  curves at  $I_{inj}=0, \pm 0.2, \pm 1.0, \pm 2.0, \pm 3.0, \pm 4.0$ , and  $\pm 8.0 \text{ mA}$  is shown



for 1.85 K and zero applied magnetic field,  $H=0$ . Here, the curve in the center is an unperturbed CVC, the upper curves are for successively increased negative  $I_{inj}$  currents, and the lower curves are for successively increased positive  $I_{inj}$  currents (the positive direction of  $I_{inj}$  and  $I_f$  is defined in the inset). The curves are successively shifted from each other (upward for  $-|I_{inj}|$  and downward for  $+|I_{inj}|$ ) by 0.02 mA along the current axis for clarity.

For  $I_{inj}$  levels in the range of 0–8 mA, the  $I_f(V_f)$  curve is altered most significantly for  $I_{inj} < 400 \mu\text{A}$ , where the coherent fraction of the current may even increase slightly (due to possible cooling effects<sup>2</sup>), although this effect is within the measurement error (estimated to be  $\pm 0.5 \mu\text{A}$  here); but then the coherent current steadily decreases for higher  $I_{inj}$ . This is better seen in the differential resistance ( $dV_f/dI_f$  versus  $V_f$ ) curves. These curves are shown for various (positive) injection levels at zero applied field in Fig. 4(b) and for  $H=35$  Oe in Fig. 4(c); curves for  $I_{inj} > 0$  are successively shifted upward from each other by four units for clarity.

One can infer from Fig. 4 that no significant change occurs in the conductivity of the Al layer when  $I_{inj}$  exceeds the foot of the “gap-difference” step, or with a further increase up to the “gap-sum” step (see curves for injection levels 2.0–6.0 mA), except for a suppression of the coherent part of the conductivity and a slight increase of the noncoherent (i.e., insensitive to a weak magnetic field) part of the conductivity in the subgap region, similar to that expected for heating. On the other hand, if a portion of the N layer sandwiched between the top and bottom S layers became superconducting [most likely, as discussed above for device 2 (cf. curve 3 in Fig. 3), the entire film would become superconducting], one would expect a dramatic change in the conductivity. Note that the  $dV_f/dI_f$  versus  $V_f$  curve has a feature [marked in Figs. 4(b) and 4(c) by arrows] that, obviously, reflects the “gap-difference” structure (cf. curve 3 in Fig. 2), but is shifted to a higher voltage in comparison with the position of the original feature in Fig. 2 due to a contribution of the normal resistance of the Al layer; this feature also does not experience dramatic changes in the  $I_{inj}$  region of interest, but smears out at higher injection currents. Summarizing these results, we conclude that for  $T > T_c$ , the Al layer does not become superconducting in the lateral direction under current injection across the SINIS structure at the  $I_{inj}$  levels where the CVC displays the anomalous “gap-difference” feature.

Given the proposed theoretical suggestions, we must ask why an enhancement of the superconductivity in Al is not observed. Within the framework of the nonequilibrium extraction mechanism,<sup>9</sup> the parameter  $\Gamma\tau_E$  should be of the order of 1 or greater, where  $\Gamma$  is an injection rate and  $\tau_E$  is an inelastic relaxation time, and the value estimated in Ref. 9 was  $\tau_E \sim 10^{-8}$  s. Since the Al layer is initially nonsuperconducting,  $\tau_E$  should correspond to the value for the normal state. An experimental study of the inelastic scattering time in Al films gives  $\tau_E \sim 10^{-9}$  s in the temperature interval of interest ( $\sim 2$ –4 K),<sup>19</sup> which yields  $\Gamma\tau_E \sim 0.1$ , i.e., too low to produce a sufficiently nonequilibrium distribution function to cause gap enhancement.

According to our estimates of the electron-phonon ( $e$ - $p$ ) and electron-electron ( $e$ - $e$ ) scattering rates in typical Al films

used in our devices,<sup>16</sup> the  $e$ - $e$  scattering increasingly dominates the  $e$ - $p$  scattering as the temperature is lowered, already starting from  $T \sim 4$  K, so that the “cooling” mechanism<sup>2,20</sup> is more appropriate to describe the experimental situation. To our knowledge, microrefrigeration using NIS and SINIS junctions has been demonstrated only at sub-Kelvin temperatures, although, theoretically, this mechanism should also work at higher temperatures. It is not clear whether this temperature limitation is due to technological or physical reasons. Another problem is to scale up the devices, because in larger junctions (with lateral dimensions of the order of 10  $\mu\text{m}$ ), heating due to quasiparticle back-tunneling from S electrodes and phonon absorption from quasiparticle pair recombination tend to overcome the cooling effect.<sup>21,22</sup> Noticeable cooling in such devices can be achieved only if special quasiparticle traps are employed.<sup>22</sup> Such a special design was not used in our devices and (to our knowledge) in the devices reported in Ref. 8.

Most importantly, junctions used for microrefrigeration (as can be deduced from parameters published, i.e., in Refs. 2 and 22) have a specific tunneling resistance in the range of  $10^{-6}$ – $10^{-5} \Omega \text{cm}^2$ , whereas the junctions that exhibit an anomalous “gap-difference” feature (described here and in Refs. 6, 8, and 14) are 10–100 times more transparent. Theoretically, the cooling power scales as  $R_t^{-1}$ , i.e., decreasing of  $R_t$  seems to be beneficial. However, in more transparent NIS (SINIS) junctions, the probability of electron tunneling below the energy gap of S increases via the Andreev reflection channel, compromising the cooling (that occurs only if electrons tunnel above the gap energy).<sup>23</sup> It is shown theoretically<sup>6</sup> that interference of normal and Andreev reflections may lead to a resonance and the formation of bound states in SINIS junctions; tunneling into a bound state in the N layer at an energy slightly below  $\Delta_{Nb}$  results in a feature in the CVC at a voltage below  $2\Delta_{Nb}/e$ , which mimics the gap-difference feature. Experimental and theoretical  $dI/dV(V)$  dependences for a junction displaying the “gap-difference” are in good agreement.<sup>6</sup> It is likely that this mechanism is realized in our devices.

#### IV. CONCLUSION

We have studied the response of the lateral conductivity of the middle Al layer in a Nb/Al/AIO<sub>x</sub>/Al/AIO<sub>x</sub>/Al/Nb (SINIS) multiterminal device to the current injected perpendicular to the layers. We did not observe any sign of superconductivity enhancement for the injection current in a region where a gap-difference-like feature is observed in the current-voltage characteristic of the SINIS device. Instead, the injection leads to suppression of the coherent part of the current and some “smearing” of the CVC of the Al layer, which may be due to heating. The gap-difference-like feature observed in the CVC of the SINIS device is possibly related to interference effects for electrons with momentum directed perpendicular to the layers. This does not mean that the enhancement of superconductivity is not possible for this device configuration, but only that special care should be taken to overcome the mechanisms leading to the opposite effect.

## ACKNOWLEDGMENTS

The authors are thankful to S. E. Shafranjuk for useful discussions and E. Goldobin for use of his GoldExi software.

This work was supported by the National Science Foundation under Grants No. EIA-0218652 and No. DMR-0509357; use was made of facilities operated by the NSF-supported Materials Research Center.

- 
- <sup>1</sup>M. Yu Kupriyanov and V. F. Lukichev, *Sov. Phys. JETP* **67**, 1163 (1988).
- <sup>2</sup>M. M. Leivo, J. P. Pekola, and D. V. Averin, *Appl. Phys. Lett.* **68**, 1996 (1996).
- <sup>3</sup>M. Yu. Kupriyanov, A. Brinkman, A. A. Golubov, M. Siegel, and H. Rogalla, *Physica C* **326-327**, 16 (1999).
- <sup>4</sup>J. Niemeyer, *Physica C* **372**, 291 (2002).
- <sup>5</sup>A. Brinkman, A. A. Golubov, H. Rogalla, F. K. Wilhelm, and M. Yu. Kupriyanov, *Phys. Rev. B* **68**, 224513 (2003).
- <sup>6</sup>I. P. Nevirkovets, S. E. Shafranjuk, and J. B. Ketterson, *Phys. Rev. B* **68**, 024514 (2003).
- <sup>7</sup>J. Kohlmann, F. Müller, R. Behr, D. Hagedorn, and J. Niemeyer, *IEEE Trans. Appl. Supercond.* **15**, 121 (2005).
- <sup>8</sup>M. G. Blamire, E. C. G. Kirk, J. E. Evetts, and T. M. Klapwijk, *Phys. Rev. Lett.* **66**, 220 (1991).
- <sup>9</sup>D. R. Heslinga and T. M. Klapwijk, *Phys. Rev. B* **47**, 5157 (1993).
- <sup>10</sup>A. V. Zaitsev, *Pis'ma Zh. Eksp. Teor. Fiz.* **55**, 66 (1992); [*JETP Lett.* **55**, 45 (1992)].
- <sup>11</sup>M. Tinkham, *Introduction to Superconductivity* (McGraw-Hill, 1996).
- <sup>12</sup>A. G. Aronov and V. L. Gurevich, *Sov. Phys. JETP* **36**, 957 (1973).
- <sup>13</sup>Yu. V. Kopaev, in *Problem of High-Temperature Superconductivity*, edited by V. L. Ginsburg and D. A. Kirzhnits (Nauka, Moscow, 1977) (in Russian).
- <sup>14</sup>I. P. Nevirkovets, *Phys. Rev. B* **56**, 832 (1997).
- <sup>15</sup>I. P. Nevirkovets, O. Chernyashevskyy, and J. B. Ketterson, *Phys. Rev. Lett.* **95**, 247008 (2005).
- <sup>16</sup>I. P. Nevirkovets, O. Chernyashevskyy, J. B. Ketterson, and E. Goldobin, *J. Appl. Phys.* **97**, 123903 (2005).
- <sup>17</sup>The possibility of an anisotropic superconducting transition temperature cannot be excluded. Evidence for such a transition in superconductor/insulator multilayers has been reported by Song and Ketterson [*Solid State Commun.* **77**, 281 (1991)].
- <sup>18</sup>V. T. Petrashov, V. N. Antonov, S. V. Maksimov, and R. Sh. Shaikhaidarov, *JETP Lett.* **58**, 49 (1993).
- <sup>19</sup>P. Santhanam and D. E. Prober, *Phys. Rev. B* **29**, R3733 (1984).
- <sup>20</sup>M. Nahum, T. M. Eiles, and J. M. Martinis, *Appl. Phys. Lett.* **65**, 3123 (1994).
- <sup>21</sup>J. Jochum, C. Mears, S. Golwala, B. Sadoulet, J. P. Castle, M. F. Cunningham, O. B. Drury, M. Frank, S. E. Labov, F. P. Lipschultz, H. Netel, and B. Neuhauser, *J. Appl. Phys.* **83**, 3217 (1998).
- <sup>22</sup>J. P. Pekola, D. V. Anghel, T. I. Suppala, J. K. Suoknuuti, A. J. Manninen, and M. Manninen, *Appl. Phys. Lett.* **76**, 2782 (2000).
- <sup>23</sup>F. Giazotto, F. Taddei, R. Fazio, and F. Beltram, *Appl. Phys. Lett.* **80**, 3784 (2002).